Electrochromic Materials

DOI: 10.1002/anie.201306162

Facile Deposition of Multicolored Electrochromic Metal–Organic Framework Thin Films**

*Casey R. Wade, Minyuan Li, and Mircea Dincă**

The construction of well-defined organic architectures on solid surfaces is a key step toward the development of more efficient and robust electronic devices. Indeed, a number of self-assembly strategies have been applied to building supramolecular structures for use in devices such as organic light-emitting diodes (OLEDs), organic transistors, and solar cells.[1–4] Recently, self-assembled coordination polymers, namely crystalline, microporous metal-organic frameworks (MOFs), have received considerable attention for their potential in a number of applications, including electronic devices.[5–9] The solvothermal methods used to synthesize MOF materials generally afford bulk single crystals or microcrystalline powders and, as a result, a number of methods have been developed to process MOFs as thin films, which are generally more desirable for use in devices.[10–18] However, MOFs still face a number of challenges in this area, particularly with regard to their insulating nature.

The incorporation of redox-active organic linkers represents one strategy toward improving the charge transport properties of MOF materials as well as imparting a response to electrochemical stimuli. In the latter case, the use of color-switching, redox-active organic linkers might be considered for the design of new, color-tunable electrochromic materials. Inorganic materials such as metal oxides and Prussian blue analogs have been extensively studied for electrochromic applications.[19,20] More recently, conducting organic polymers such as polythiophenes have received considerable attention owing to their greater color tunability and efficiency, and faster switching times.[21,22] Despite significant advances, the need still exists for more easily synthesized and processable electrochromic materials with the same or greater degree of tunability. In this sense, the well-defined structures, self-assembly synthesis, and guest-accessible microporosity of MOFs might prove useful for their application in this field.

Herein, we describe the solvothermal deposition and electrochemical properties of porous, micron-thick Zn-pyrazolate MOF films containing redox-active naphthalene diimide (NDI) linkers. NDIs have been extensively studied for their electron accepting properties which make them attractive as n-type semiconductors.[23,24] Furthermore, core substitution of NDIs with electron donor groups results in the appearance of charge-transfer transitions in the visible spectrum, affording color-tunable and sometimes fluorescent dyes with applications in optoelectronics and sensing.[25–36] A handful of MOFs containing NDI-based linkers have been reported[37–39] and studied as gas sorption,[40,41] photochromic,[37,39] and fluorescent sensor materials.[42,43] However, studies of their electrochemical properties remain scarce.[37,44] Here, we show that processing them as homogeneously dispersed thin films enables their use as multicolored electrochromic devices.

Our group has been concerned with developing modular syntheses for water-stable pyrazolate-based MOFs, and recently we described a series of core-substituted NDI-based materials.[45] These MOFs (Zn(NDI-X), Figure 1) were obtained as microcrystalline powders by heating 1.1:1

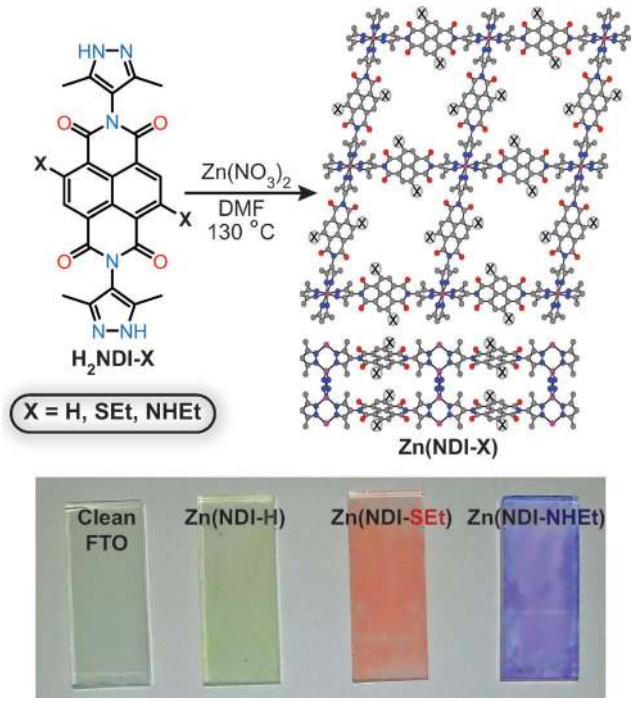

Figure 1. Top: Synthesis and simulated structure of Zn(NDI-X) (X = H, NHEt, and SEt). Bottom: Optical images of macroscopic films of Zn(NDI-X) on FTO.

[*] Dr. C. R. Wade, M. Li, Prof. M. Dincă
Department of Chemistry
Massachusetts Institute of Technology
77 Massachusetts Avenue, Cambridge, MA, 02139 (USA)
E-mail: mdinca@mit.edu
Homepage: http://web.mit.edu/dincalab

[**] This work was supported by the U.S. Department of Energy, Office of Science, Office of Basic Energy Sciences under award number DE-SC0006937. This work also made use of the MRSEC Shared Experimental Facilities at MIT, supported in part by the NSF under award number DMR-0819762. M.D. thanks 3M for summer funding from a non-tenured faculty award and the MIT-Hayashi Fund for a travel grant.

Supporting information for this article is available on the WWW under http://dx.doi.org/10.1002/anie.201306162.

molar mixtures of $Zn(NO_3)_2{\cdot}6H_2O$ and H_2NDI-X (X = H, S-C_2H_5, NH-C_2H_5) in *N*,*N*-dimethylformamide (DMF) at 130 °C. The resulting products precipitated as fine powders, which uniformly coated the walls of the glass reaction vessel. This observation suggested fast nucleation of these materials, and we surmised that these conditions might be used to enable the formation of homogeneous thin films for electrochemical applications. Accordingly, precleaned fluorine-doped tin oxide (FTO)-coated glass substrates were placed into reaction mixtures similar to those used to prepare the Zn(NDI-X) MOFs, and the mixtures were heated at 130 °C for 4 h. Upon cooling, the FTO substrates were removed and rinsed with DMF, revealing the presence of highly colored films attached to the surface (Figure 1). The strong adhesion of these films to the substrate surface was demonstrated by their resilience to washing with a number of organic solvents (acetone, ethanol, DMF) as well as sonication in DMF. As shown in Figure 2a, powder X-ray diffraction measurements

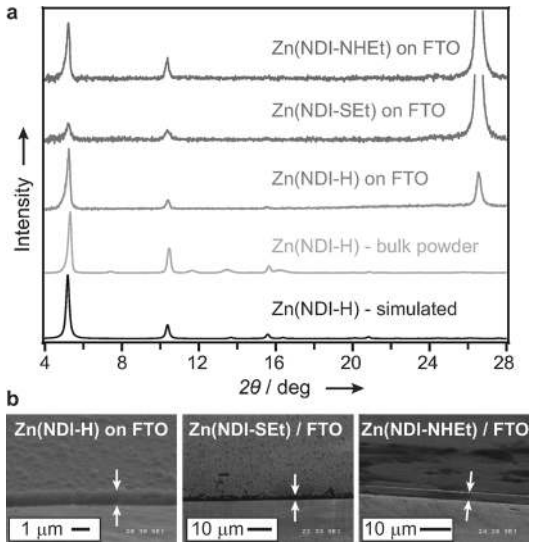

Figure 2. a) Powder X-ray diffraction patterns of Zn(NDI-X) (X = H, NHEt, and SEt) films on FTO substrates after washing (see the Supporting Information for details) and the bulk powder sample of Zn(NDI-H) for comparison. The prominent peak at $2\theta = 26.5°$ corresponds to SnO_2 from the FTO substrate. b) Scanning electron micrographs of the Zn(NDI-X) films. White arrows indicate the surface of the MOF films and their contact with the FTO plate.

on the FTO substrates revealed the presence of diffraction peaks corresponding to the (110), (220), and (330) reflections of the Zn(NDI-X) MOF bulk powders. Substrates treated under similar conditions in DMF solutions of the ligand, but in the absence of $Zn(NO_3)_2$, showed no visible film growth or diffraction peaks corresponding to ligand deposition (Figure S1). Together, these results support the formation of Zn(NDI-X) MOF films using relatively simple solvothermal conditions. Indeed, scanning electron micrographs (SEMs) of the FTO substrates showed uniform coverage of about 1 μm-thick Zn(NDI-X) films in all three cases (X = H, SEt, NHEt).[46] In fact, no distinct particles could be observed by SEM, suggesting the presence of evenly packed crystallites less than 10 nm in diameter (Figure 2b).

Encouraged by the strong adhesion and remarkable uniformity of the pyrazolate MOF films on conductive FTO substrates, we sought to explore their electrochemical and electrochromic behaviors. Cyclic voltammetry (CV) measurements were carried out in DMF solutions containing 0.1 M $[(n\text{Bu})_4\text{N}]PF_6$ using a three-electrode electrochemical cell with the FTO thin film as the working electrode, platinum mesh as the counter electrode, and a Ag/Ag(cryptand)$^+$ reference electrode. As shown in Figure 3, all three films

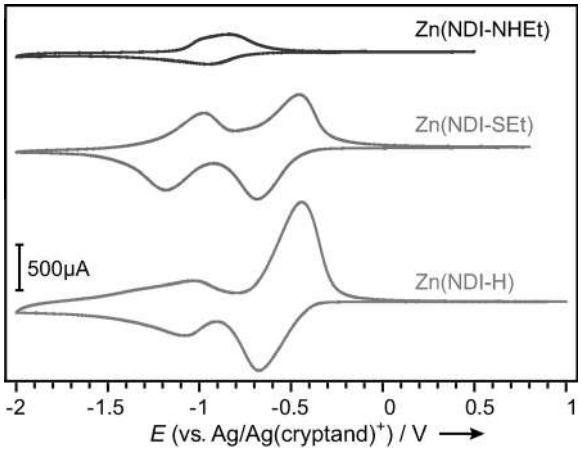

Figure 3. Cyclic voltammograms of Zn(NDI-X) (X = H, NHEt, and SEt) films on FTO substrates measured in DMF solution containing 0.1 M $[(n\text{Bu})_4\text{N}]PF_6$ at a scan rate of 50 mV s^{-1}.

exhibited well-behaved redox events. The Zn(NDI-H) film showed two quasi-reversible processes at $E_{1/2} = -0.56$ V and -1.05 V, which are consistent with the reported $[NDI]^{0/\bullet-}$ and $[NDI]^{\bullet-/2-}$ redox couples, respectively.[47] The observed peak separations (ΔE_p of 230 mV for $[NDI]^{0/\bullet-}$ and 50 mV for $[NDI]^{\bullet-/2-}$ at 50 mV s^{-1} scan rate) as well as the peak current versus scan rate dependence suggest electron diffusion or mass transfer limitations within the film, as might be expected for porous, nonconductive films (see Supporting Information for additional details). Solution CV measurements on the free ligand H_2NDI-H using a glassy carbon button electrode showed fully reversible $[H_2NDI\text{-}H]^{0/\bullet-}$ and $[H_2NDI\text{-}H]^{\bullet-/2-}$ redox processes at $E_{1/2} = -0.44$ and -0.97 V, respectively (Table 1, Figure S2). The slight cathodic shifts of the NDI reductions in the MOF film (approximately 100 mV) relative to the free ligand are consistent with greater negative charge

Table 1: Measured redox potentials for Zn(NDI-X) thin films and ligands.

	$[NDI\text{-}X]^{0/\bullet-}$ [V][b]		$[NDI\text{-}X]^{\bullet-/2-}$ [V][b]	
Zn(NDI-X)	$E_{1/2}$	(ligand $E_{1/2}$)	$E_{1/2}$	(ligand $E_{1/2}$)
H	−0.56	(−0.44)	−1.05	(−0.97)
SEt	−0.57	(−0.49)	−1.08	(−0.99)
NHEt[a]	−0.90	(−0.72)		(−1.25)

[a] An irreversible ligand oxidation was also observed at $E_a = +1.15$ V; [b] All potentials are measured versus a Ag/Ag(cryptand)$^+$ reference electrode.

density of the doubly deprotonated ligand in the MOF framework. Notably, the Zn(NDI-H) film also showed excellent stability toward electrochemical cycling with no decrease in the peak current observed over 25 cycles at a scan rate of 100 mV s^{-1} (Figure S3).

Similar to Zn(NDI-H), the Zn(NDI-SEt) film showed two quasi-reversible reduction waves at −0.57 and −1.08 V which were cathodically shifted from those of the free ligand H_2NDI-SEt (−0.49 V and −0.99 V, respectively). The Zn(NDI-NHEt) film displayed a single poorly defined, but moderately reversible, reduction at −0.90 V. The presence of a single reduction wave in this film was unexpected since the H_2NDI-NHEt ligand showed reversible $[H_2NDI\text{-}NHEt]^{0/\bullet-}$ and $[H_2NDI\text{-}NHEt]^{\bullet-/2-}$ couples at −0.72 and −1.25 V, respectively. While likely attributable to effects from framework immobilization of the ligand, the exact origin of this behavior has not been determined. The cathodic shifts in the reduction potentials moving from X = H to SEt to NHEt are in agreement with the incorporation of increasingly electron-rich substituents at the NDI core.[48] The Zn(NDI-SEt) and Zn(NDI-NHEt) films also exhibited contrasting behavior over multiple CV scans. Whereas Zn(NDI-H) exhibited excellent stability upon cycling, the peak current for Zn(NDI-SEt) steadily increased over the course of 50 cycles before reaching a plateau (Figure S4). We assign this behavior to "crowding" of the MOF channels by the SEt groups, which reduces the pore diameter and impedes electrolyte diffusion into the structure resulting in an "electrochemical conditioning" period. Notably, soaking the Zn(NDI-SEt) film in an electrolyte solution prior to running CV measurements did not eliminate the need for a conditioning period, perhaps indicating that electrolyte $[(n\text{Bu})_4\text{N}]PF_6$ diffusion into the neutral framework is unfavorable in the absence of an electric bias. In further contrast, the Zn(NDI-NHEt) film displayed a small, but continual decrease in peak current over 25 cycles (Figure S5) which we attribute to film delamination based on visual inspection of the FTO plate after cycling. We note, however, that electrolyte solutions tested by CV with a clean working electrode showed no indication of free ligand in solution, suggesting that the MOF may delaminate intact rather than by dissolution. Furthermore, PXRD diffraction measurements confirmed that the crystallinity of all three MOF films was retained after CV (Figure S6).

During electrochemical cycling, we observed striking color changes at the MOF film electrodes which coincided with the reduction events (Figure S7). Because of the transparency of the thin Zn(NDI-X) films, we considered that these changes might be monitored using transmission UV/Vis spectroscopy. Indeed, UV/Vis spectra could easily be obtained by suspending the Zn(NDI-X) films in DMF, and the measured spectra closely matched those of the dissolved ligands in the same solvent (Figures S8, S9, and S10). Consequently, the UV/Vis spectra of the Zn(NDI-X) films were measured at regular intervals during the cathodic sweep (0 → −1.75 V vs. Ag/Ag(cryptand)$^+$) of CV scans run at a scan rate of 10 mV s^{-1}.

Within the 0 → −1.75 V scan window, the UV/Vis spectra of the Zn(NDI-H) and Zn(NDI-SEt) films exhibited changes characteristic of the formation of $[NDI\text{-}X]^{\bullet-}$ and $[NDI\text{-}X]^{2-}$ species (Figure 4a,b).[35,47,49,50] From 0 → −1.0 V, the disappearance of π–π* transitions around $\lambda_{max} \approx 360$–380 nm concomitant with the appearance of new intense absorptions around $\lambda_{max} \approx 470$–490 nm indicate the formation of $[NDI\text{-}X]^{\bullet-}$ species. Moreover, the observed darkening of the films over this potential range may be attributed to the appearance of new absorption bands farther into the visible region. Upon scanning to −1.75 V, further changes resulting in a second set of isosbestic points suggested the formation of $[NDI\text{-}X]^{2-}$ species. Over this range, the absorption bands with $\lambda_{max} \approx 470$–490 nm gradually decreased while a new pair of bands appeared around $\lambda_{max} \approx 400$–435 nm and absorption bands in

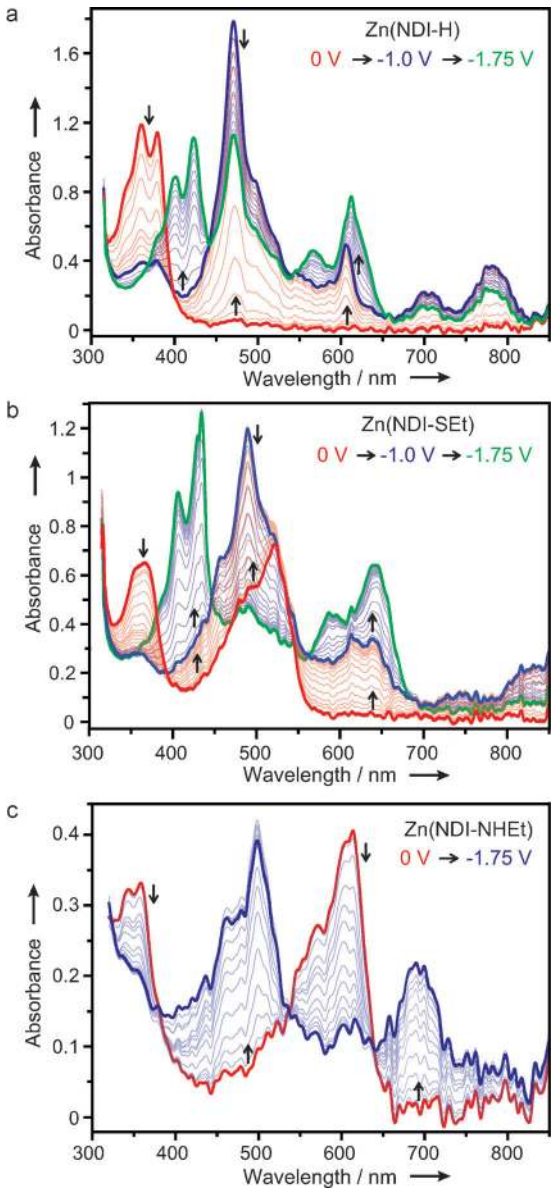

Figure 4. Spectroelectrochemical data collected by transmission UV/Vis spectroscopy for Zn(NDI-X) [X = H (a), SEt (b), and NHEt (c)] films on FTO substrates in DMF solution containing 0.1 M $[(n\text{Bu})_4\text{N}]PF_6$. UV/Vis absorption spectra were collected at 6 s intervals during the cathodic scan (10 mV s^{-1}) of a CV measurement. All potentials are measured versus a Ag/Ag(cryptand)$^+$ reference electrode.

the 550–650 nm region gained intensity. The decrease in absorbance in the 500 nm region over this potential range should be responsible for the transition in the observed color of the films from brown to green. Changes in the UV/Vis spectrum of the Zn(NDI-NHEt) film over the potential range $0 \rightarrow -1.75$ V are consistent with the CV data, indicating the formation of only the singly reduced $[NDI\text{-}NHEt]^{\bullet-}$ species. This is supported by the presence of a single set of isosbestic points owing to the disappearance of the π–π^* transitions ($\lambda_{max} = 343$ nm, 358 nm) and the appearance of new bands with $\lambda_{max} = 461$, 498, and 690 nm.

The coloration efficiency (CE), the ratio of the absorbance change to the charge injected per unit electrode area, provides a useful metric for evaluating the power requirements of electrochromic materials. Common inorganic electrochromic materials such as metal oxides typically exhibit lower CEs than conductive organic polymers such as polythiophenes, which generally display efficiencies much greater than 100 $cm^2\,C^{-1}$.[51–54] The calculated CEs for the Zn(NDI-X) films were found to be > 100 $cm^2\,C^{-1}$ in the blue region of the spectrum ($\lambda = 470$–500 nm) where large absorption bands appeared upon reduction at -1.0 V (Table S2). Slightly lower CE values in the 60–90 $cm^2\,C^{-1}$ range were calculated for absorption bands in the visible region from 600–700 nm. These values suggest that the efficiency of the Zn(NDI-X) electrochromic films is comparable to common electrochromic organic polymers.

In the foregoing results, we demonstrate the facile deposition of strongly adhering, homogeneous, and crystalline thin films of a series of pyrazolate MOFs. We hypothesize that the ease with which these films form is due to fast nucleation of MOF crystallites driven by the formation of strong metal–ligand bonds. This behavior may prove generalizable to the wider class of water-stable frameworks, a possibility that we are currently investigating. Furthermore, the use of NDI-based ligands to deposit MOFs on conductive FTO surfaces affords electroactive films which exhibit fast and reversible color switching. Given the inherent porosity, color tunability, and reversible redox behavior of such films, we envision that they might serve as active materials for electrochromic windows or competent host materials for electrochemical cation insertion, areas which we are also currently pursuing.

Received: July 16, 2013
Revised: August 16, 2013
Published online: October 16, 2013

Keywords: electrochemistry · electrochromic materials · metal–organic frameworks · naphthalene diimide · thin films

[1] M. R. Wasielewski, *Acc. Chem. Res.* **2009**, *42*, 1910 – 1921.
[2] F. Würthner, K. Meerholz, *Chem. Eur. J.* **2010**, *16*, 9366 – 9373.
[3] D. M. Bassani, L. Jonusauskaite, A. Lavie-Cambot, N. D. McClenaghan, J.-L. Pozzo, D. Ray, G. Vives, *Coord. Chem. Rev.* **2010**, *254*, 2429 – 2445.
[4] R. Bhosale, J. Mísek, N. Sakai, S. Matile, *Chem. Soc. Rev.* **2010**, *39*, 138 – 149.
[5] G. Lu, J. T. Hupp, *J. Am. Chem. Soc.* **2010**, *132*, 7832 – 7833.
[6] M. D. Allendorf, A. Schwartzberg, V. Stavila, A. A. Talin, *Chem. Eur. J.* **2011**, *17*, 11372 – 11388.
[7] T. C. Narayan, T. Miyakai, S. Seki, M. Dincă, *J. Am. Chem. Soc.* **2012**, *134*, 12932 – 12935.
[8] L. Sun, T. Miyakai, S. Seki, M. Dincă, *J. Am. Chem. Soc.* **2013**, *135*, 8185 – 8188.
[9] Y. Kobayashi, B. Jacobs, M. D. Allendorf, J. R. Long, *Chem. Mater.* **2010**, *22*, 4120 – 4122.
[10] O. Shekhah, J. Liu, R. A. Fischer, C. Wöll, *Chem. Soc. Rev.* **2011**, *40*, 1081 – 1106.
[11] A. Bétard, R. A. Fischer, *Chem. Rev.* **2012**, *112*, 1055 – 1083.
[12] O. Shekhah, H. Wang, S. Kowarik, F. Schreiber, M. Paulus, M. Tolan, C. Sternemann, F. Evers, D. Zacher, R. A. Fischer, C. Wöll, *J. Am. Chem. Soc.* **2007**, *129*, 15118 – 15119.
[13] R. Makiura, S. Motoyama, Y. Umemura, H. Yamanaka, O. Sakata, H. Kitagawa, *Nat. Mater.* **2010**, *9*, 565 – 571.
[14] B. Liu, M. Tu, R. A. Fischer, *Angew. Chem.* **2013**, *125*, 3486 – 3489; *Angew. Chem. Int. Ed.* **2013**, *52*, 3402 – 3405.
[15] R. Ameloot, L. Stappers, J. Fransaer, L. Alaerts, B. F. Sels, D. E. De Vos, *Chem. Mater.* **2009**, *21*, 2580 – 2582.
[16] P. Horcajada, C. Serre, D. Grosso, C. Boissière, S. Perruchas, C. Sanchez, G. Férey, *Adv. Mater.* **2009**, *21*, 1931 – 1935.
[17] A. Schoedel, C. Scherb, T. Bein, *Angew. Chem.* **2010**, *122*, 7383 – 7386; *Angew. Chem. Int. Ed.* **2010**, *49*, 7225 – 7228.
[18] M. Li, M. Dincă, *J. Am. Chem. Soc.* **2011**, *133*, 12926 – 12929.
[19] G. A. Niklasson, C. G. Granqvist, *J. Mater. Chem.* **2007**, *17*, 127 – 156.
[20] R. J. Mortimer, *Annu. Rev. Mater. Sci.* **2011**, *41*, 241 – 268.
[21] G. Sonmez, *Chem. Commun.* **2005**, 5251 – 5259.
[22] C. M. Amb, A. L. Dyer, J. R. Reynolds, *Chem. Mater.* **2011**, *23*, 397 – 415.
[23] X. Zhan, A. Facchetti, S. Barlow, T. J. Marks, M. A. Ratner, M. R. Wasielewski, S. R. Marder, *Adv. Mater.* **2011**, *23*, 268 – 284.
[24] F. Würthner, M. Stolte, *Chem. Commun.* **2011**, *47*, 5109 – 5115.
[25] C. Röger, F. Wuerthner, *J. Org. Chem.* **2007**, *72*, 8070 – 8075.
[26] S. V. Bhosale, C. H. Jani, S. J. Langford, *Chem. Soc. Rev.* **2008**, *37*, 331 – 342.
[27] T. D. M. Bell, S. Yap, C. H. Jani, S. V. Bhosale, J. Hofkens, F. C. De Schryver, S. J. Langford, K. P. Ghiggino, *Chem. Asian J.* **2009**, *4*, 1542 – 1550.
[28] J. Mísek, A. V. Jentzsch, S. Sakurai, D. Emery, J. Mareda, S. Matile, *Angew. Chem.* **2010**, *122*, 7846 – 7849; *Angew. Chem. Int. Ed.* **2010**, *49*, 7680 – 7683.
[29] C.-C. Lin, M. Velusamy, H.-H. Chou, J. T. Lin, P.-T. Chou, *Tetrahedron* **2010**, *66*, 8629 – 8634.
[30] N. Sakai, J. Mareda, E. Vauthey, S. Matile, *Chem. Commun.* **2010**, *46*, 4225 – 4237.
[31] C. Zhou, Y. Li, Y. Zhao, J. Zhang, W. Yang, Y. Li, *Org. Lett.* **2011**, *13*, 292 – 295.
[32] A. Pron, R. R. Reghu, R. Rybakiewicz, H. Cybulski, D. Djurado, J. V. Grazulevicius, M. Zagorska, I. Kulszewicz-Bajer, J.-M. Verilhac, *J. Phys. Chem. C* **2011**, *115*, 15008 – 15017.
[33] R. P. Cox, H. F. Higginbotham, B. A. Graystone, S. Sandanayake, S. J. Langford, T. D. M. Bell, *Chem. Phys. Lett.* **2012**, *521*, 59 – 63.
[34] S. Guo, W. Wu, H. Guo, J. Zhao, *J. Org. Chem.* **2012**, *77*, 3933 – 3943.
[35] S. Guha, F. S. Goodson, L. J. Corson, S. Saha, *J. Am. Chem. Soc.* **2012**, *134*, 13679 – 13691.
[36] H. F. Higginbotham, R. P. Cox, S. Sandanayake, B. A. Graystone, S. J. Langford, T. D. M. Bell, *Chem. Commun.* **2013**, *49*, 5061 – 5063.
[37] S. Brochsztain, M. A. Rodrigues, G. J. F. Demets, M. J. Politi, *J. Mater. Chem.* **2002**, *12*, 1250 – 1255.
[38] B.-Q. Ma, K. L. Mulfort, J. T. Hupp, *Inorg. Chem.* **2005**, *44*, 4912 – 4914.

[39] L. Han, L. Qin, L. Xu, Y. Zhou, J. Sun, X. Zou, *Chem. Commun.* **2013**, *49*, 406 – 408.
[40] K. L. Mulfort, J. T. Hupp, *J. Am. Chem. Soc.* **2007**, *129*, 9604 – 9605.
[41] K. L. Mulfort, T. M. Wilson, M. R. Wasielewski, J. T. Hupp, *Langmuir* **2009**, *25*, 503 – 508.
[42] Y. Takashima, V. M. Martínez, S. Furukawa, M. Kondo, S. Shimomura, H. Uehara, M. Nakahama, K. Sugimoto, S. Kitagawa, *Nat. Commun.* **2011**, *2*, 168.
[43] V. Martínez-Martínez, S. Furukawa, Y. Takashima, I. López Arbeloa, S. Kitagawa, *J. Phys. Chem. C* **2012**, *116*, 26084 – 26090.
[44] P. M. Usov, C. Fabian, D. M. D'Alessandro, *Chem. Commun.* **2012**, *48*, 3945 – 3947.
[45] C. R. Wade, T. Corrales-Sanchez, T. C. Narayan, M. Dincă, *Energy Environ. Sci.* **2013**, *6*, 2172 – 2177.
[46] We have not optimized the synthetic parameters to obtain 1 μm-thick films. However, using the conditions described in the Supporting Information, we consistently obtain films of this thickness.
[47] G. Andric, J. F. Boas, A. M. Bond, G. D. Fallon, K. P. Ghiggino, C. F. Hogan, J. A. Hutchison, M. A.-P. Lee, S. J. Langford, J. R. Pilbrow, G. J. Troup, C. P. Woodward, *Aust. J. Chem.* **2004**, *57*, 1011 – 1019.
[48] C. Thalacker, C. Röger, F. Würthner, *J. Org. Chem.* **2006**, *71*, 8098 – 8105.
[49] S. Chopin, F. Chaignon, E. Blart, F. Odobel, *J. Mater. Chem.* **2007**, *17*, 4139 – 4146.
[50] See Figures S8, S9, and S10 of the Supporting Information for comparison of the UV/Vis spectra of the electrochemically reduced Zn(NDI-X) films with those of the chemically reduced ligands (H_2NDI-X) in DMF solution.
[51] C. G. Granqvist, *Sol. Energy Mater. Sol. Cells* **2000**, *60*, 201 – 262.
[52] C. L. Gaupp, D. M. Welsh, R. D. Rauh, J. R. Reynolds, *Chem. Mater.* **2002**, *14*, 3964 – 3970.
[53] G. Sonmez, H. Meng, F. Wudl, *Chem. Mater.* **2004**, *16*, 574 – 580.
[54] R. J. Mortimer, J. R. Reynolds, *J. Mater. Chem.* **2005**, *15*, 2226 – 2233.

